Reprocessing strategy to obtain quantitative early time data from historic VTEM surveys

James Macnae*
RMIT University School of Applied Sciences
GPO Box 2476, Melbourne, Vic 3001
James.macnae@rmit.edu.au

Stuart Baron-Hay
Geotech Airborne (Pty.) Ltd.
29 Mulgul Rd, Malaga WA 6090
stuart.baron-hay@geotechairborne.com.au

SUMMARY

While data in AEM systems such as VTEM is continuously sampled at 5 or 10 microsecond intervals, conventional processing steps in the past have not provided useful data close to transmitter current turnoff. In historic VTEM data for example, delivered data usually starts many tens or even a hundred microseconds or so after turnoff. Experiments in deconvolution of early time data at high altitude identified that the symptoms of "problem" early-time data were that the underlying cause had a linear phase response, resulting in a consistent "system" exponential response in time-domain. This unwanted or spurious response is experimentally determined to be of variable amplitude, and of either sign, usually reducing the data at early delays, but occasionally enhancing the combined response. A change in processing strategy to specifically identify and subtract this additive spurious response from a valid earth response has led to the extraction of quantitative AEM data at early delays in the 10 to 20 µs range. The process can be applied to historic data. System bandwidth limitations do of course provide a limit to the accurate sampling of the earth response at extremely early delays. More recently, hardware changes have increased the system bandwidth and reduced the need for software corrections to acquired data.

Key words: bandwidth, early-time, airborne, electromagnetic

INTRODUCTION

This research had the aim of developing processes to provide quantitative, early-time data for the VTEM system. The data delivered to clients by contractor Geotech, operators of the VTEM system, usually start at delay times between 30 to 110 microseconds, depending on details of the specific system and flying conditions. Earlier (and zero-delay) time data was collected at 5 or 10 microsecond resolution, but not delivered due to its incompatibility with quantitative expectation.

Early-time or high-frequency AEM data is desirable for shallow sounding or mapping of resistive areas (Spies and Frischknecht 1991). The shallower the depth of interest, or the more resistive the geology, the more important such data becomes (Huang and Fraser 2002). Many airborne electromagnetic (AEM) systems have problems in getting quantitative early-time data, due to a number of issues including bandwidth (Effersø et al. 1999). Efferso et al. suggested processing means to correct for bandwidth limitations using imperfect data.

An established processing strategy to correct for system imperfections such as bandwidth limitation is to deconvolve measured responses in frequency domain to get an ideal response. This approach usually requires a streamed current monitor and streamed receiver data, and was first proposed by (Annan 1986) for the prototype Prospect AEM system, and implemented in the fixed-wing Spectrem (Leggatt 1996), Saltmap (Duncan et al. 1992) and Tempest (Lane et al. 1998) systems.

Deconvolution in theory is a simple procedure that will correct one complete period for linear system imperfections including transmitter current drift through the following operation:

$$R(t) \Leftrightarrow \mathbf{R}(\omega) = \frac{\mathbf{C_0}(\omega)\ \mathbf{B}(\omega)}{\mathbf{C}(\omega)\ \mathbf{H_0}(\omega)}\ \mathbf{W}(\omega) \qquad (1)$$

Where $R(t)$ is the desired response (corresponding to $\mathbf{R}(\omega)$ in frequency domain), C is the instantaneous current monitor and C_0 the averaged high altitude reference current monitor measurement, B the instantaneous survey data and H_0 the averaged high-altitude data respectively. $W(t)$ is an ideal waveform for which the response is desired. This formula does not correct for non-linear effects or receiver drift. In general, quantitative predictions of R are best when W is close to the reference waveform H_0 .The method is virtually perfect for small bandwidth corrections and transmitter drift.

In practice, there are a number of important considerations that require attention to ensure numerical stability, such as background removal and zero drift correction prior to FFT. Other requirements are that filtering and division processes are applied only to odd harmonics derived from processing one full waveform whose exact antisymmetry has been ensured, and avoiding/correcting at frequencies of powerline and VFL communication signals. As well, the deconvolution methodology can be used to extract B from measured dB/dt responses.

Deconvolution has been applied to fixed wing AEM systems as discussed, and this research initially investigated the application of deconvolution to VTEM bin files, short segments of streamed data collected for calibration purposes.

METHOD AND RESULTS

Prior to 2010, streamed VTEM data was only collected in short bursts (of 1 to 2 second duration), and usually only at high-altitude for the purpose of defining a reference waveform. A monitor measured *dA/dt*, the time derivative of transmitted current, and *dB/dt*, the response from a receiver, with 5 example waveforms from one high-altitude burst shown in Figure 1. Streamed data at survey height over deep seawater was also available.

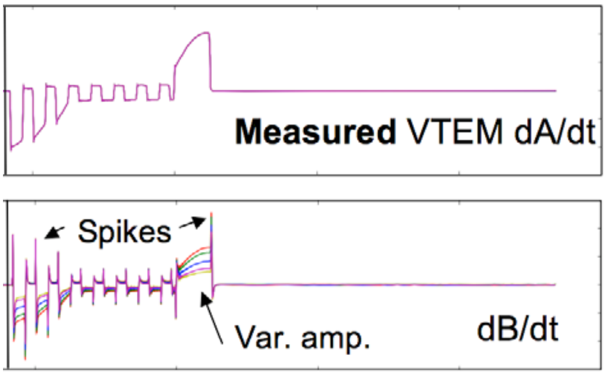

Figure 1: Comparison of 5 sample high-altitude waveforms leaving transmitter *(dA/dt)* and received waveforms *(dB/dt)*. All *dA/dt* waveforms have identical amplitude and shape. As well as received *dB/dt* having a variable amplitude component of *dA/dt* due to imperfect bucking, there are additional double spikes seen in *dB/dt* at every step in *dA/dt.*

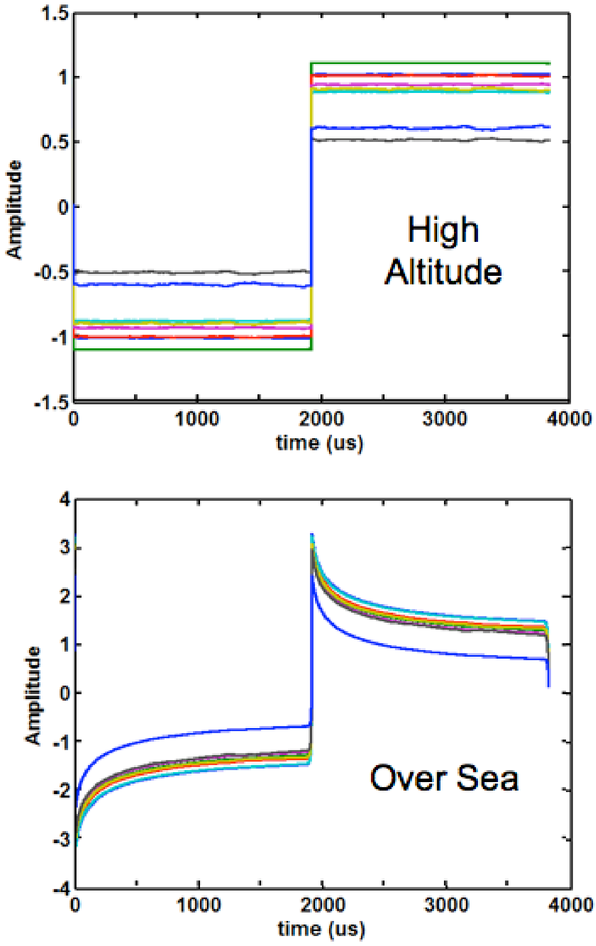

Figure 2: Example streamed VTEM *dA/dt* and *dB/dt* data deconvolved to step-response at high altitude and at survey altitude over deep seawater

An average of the high-altitude data was used to make reference waveforms corresponding to C_0 and H_0 in equation (1). The streamed data were then deconvolved with a target waveform being a 100% duty-cycle step response and the results shown in Figure 2. While the high altitude data has the appearance of a square-wave, and the seawater data the appearance of a monotonic decay, when looked at in detail (Figure 3) there are several unusual features in the predicted step response.

Firstly, there appears to be a response prior to the (predicted) step excitation, which response cannot be "causal". For the high-altitude data, and the response prior to the step for seawater, the behaviour closely matched an exponential rise (before) or exponential decay (after), with constant $\tau 0$ of about 20 µs.

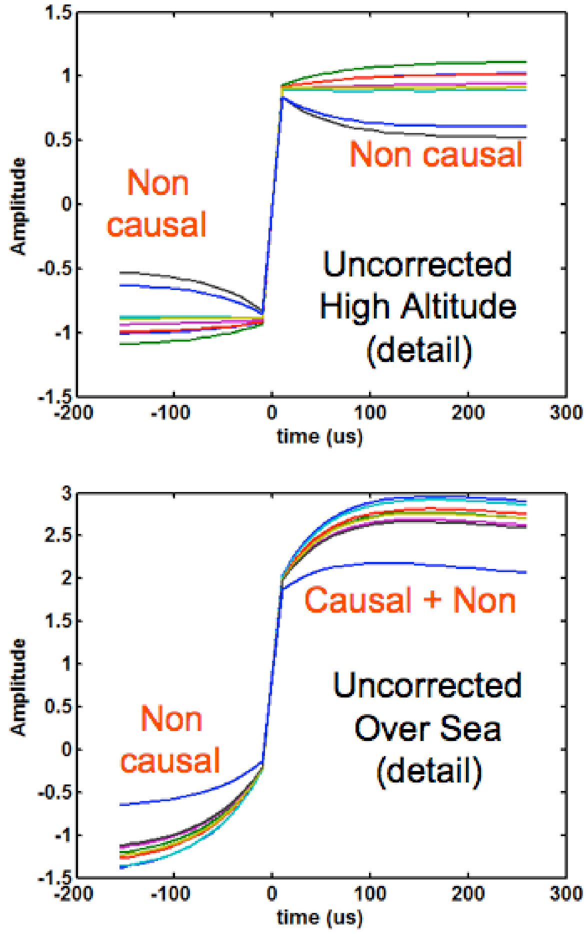

Figure 3: Detail near the step transition showing time-shifting (non-causal) effects before the transition. The non-causal part has linear phase in frequency domain and exponential behaviour in time-domain.

It was recognised in frequency domain that the non-causal component of the response had linear phase, which implies that it has a (very small and variable) time-shift between instantaneous and reference waveforms, modified with a single pole (exponential $\tau 0$) response. As a result, the mirror image of the response prior to the step can be used to subtract from the data after the step, in the process removing this non-causal component. Figure 4 presents the results of this correction on high-altitude and seawater data.

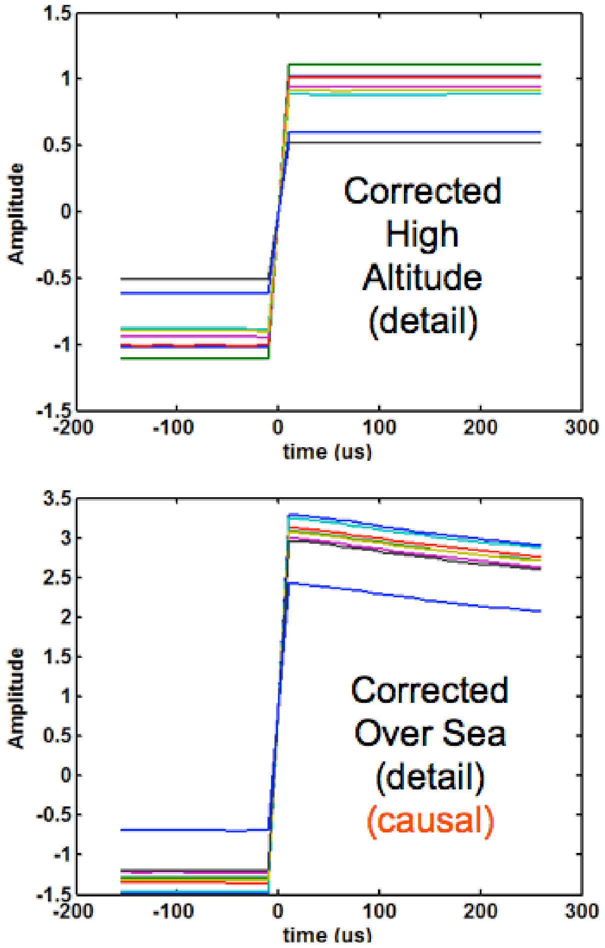

Figure 4: Data corrected using the exponential response prior to the transition. The residual response is now causal and has the decay characteristics expected. Deconvolution has produced quantitative data at 10 us after the step.

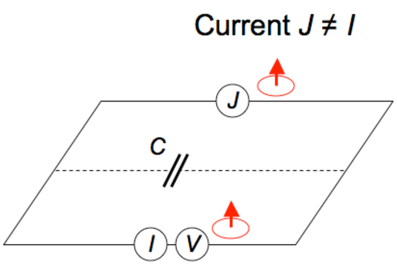

Figure 5: Capacitance across the transmitter loop in ground fixed-transmitter surveys causes current *J* at the back of a large transmitter loop to be different from that leaving the transmitter. Wire currents may be measured with a standard *dB/dt* receiver (red) operated either side of the wire.

Current "leakage" through capacitance has been seen in large ground loops used in UTEM surveys (Kurtz et al. 1989). Essentially, high-frequency energy is short-circuited through the antenna effect, and the current *J* at the back of a loop (Figure 5) is different from the current leaving the transmitter by the displacement current through the distributed capacitance *C* between the opposite sides of the loop. We believe that the same effect is affecting the received signal in VTEM data, causing the bucking current *B* to be slightly different from the main transmitter current *T*. The receiver senses the difference between the (approximately equal amplitude) fields of *B* and *T*, which difference contains impulsive excitations that then decay through the *RC* damping of known τ.

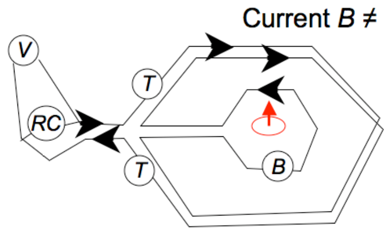

Figure 6: Schematic of a bucked AEM transmitter and central receiver. A voltage source *V* in the aircraft drives current *T* around a multi-turn transmitter loop, with a small, reversed (bucking) loop carrying current *B* ≈*T*. A damping resistor *R* and (lumped) parasitic capacitance *C* are shown in the circuit, and have time constant $\tau 0$. In fact, the parasitic capacitance is distributed between the main and bucking loop windings.

Because historical VTEM systems only recorded windowed channels on survey, we investigated if knowledge from deconvolution could be used to improve such windowed data.

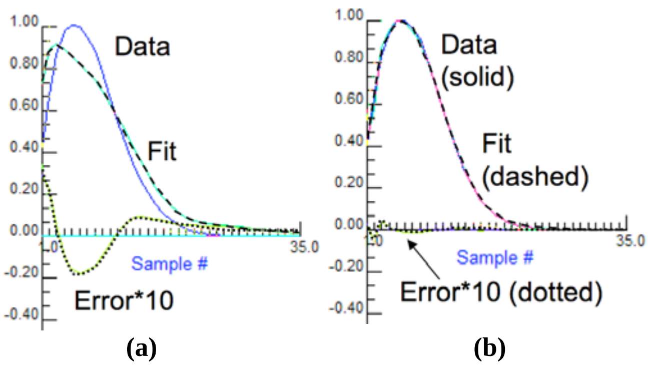

Figure 7: (VTEM survey data (solid) and "best fit" response (dashed) to data (Sample 1 at 10 us)) through Sample 6 (100 ms) to Sample 35 (10 ms). The rms error of fit exceeds 7% for the fit (a) to standard data, and is less than 0.2% if (b) parasitic capacitance is included. .

Figure 7 shows VTEM data from 10 us to 10 ms, together with a best fit layered-earth decay from program EMFlow (Macnae et al. 1998). When a parasitic capacitance effect is included (exponential rise of time constant $\tau 0$, convolved with the received primary waveform *dB/dt*) in the basis functions for fitting, the rms error of fit is reduced to less than 0.2%. This parasitic response has amplitude much larger than the constituent components of the layered earth decay (Figure 8) Next the parasitic response can be subtracted from the data, leaving an "uncontaminated" response, which since it has not been deconvolved may show the band-liming constraints of transmitter and receiver circuitry.

EMFlow processing of corrected data leads to far more coherent responses at shallow depths than processing using standard data as delivered. Figure 10 shows comparison maps of conductivity in the top 10 m from a survey in Africa, derived from CDI sections created from corrected and uncorrected data. The lower left portion of the map is fairly resistive, and its response only evident at early delay times. Correction of the data has allowed for a) far greater coherence in both conductive and resistive areas and b) the reliable detection of poorly conducting linear features in the resistive zone.

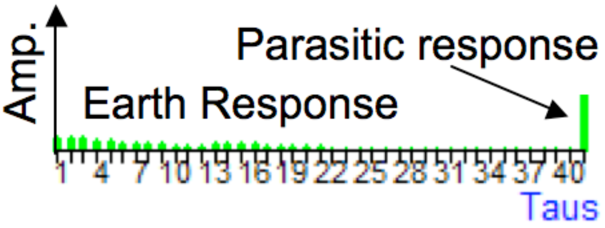

Figure 8: The distributed amplitude of the 40 basis function used to fit a layered-earth response, plus the large parasitic response amplitude at position 41 on the horizontal axis.

CONCLUSIONS

Experiments in deconvolution of early time data at high altitude identified that the symptoms of "problem" early-time data were that the underlying cause had a linear phase response, resulting in a consistent "system" exponential response in time-domain. This unwanted or spurious response is experimentally determined to be of variable amplitude, and of either sign, usually reducing the data at early delays, but occasionally enhancing the combined response. A change in processing strategy to specifically identify and subtract this additive spurious response from a valid earth response has led to the extraction of quantitative AEM data at early delays in the 10 to 20 μs range. The process can be applied to historic data. System bandwidth limitations do of course provide a limit to the accurate sampling of the earth response at extremely early delays.

ACKNOWLEDGMENTS

We thank Geotech Airborne Limited for support of this research, and CD3D for permission to use the field data.

REFERENCES

Annan, A.P. 1986. Development of the PROSPECT I airborne electromagnetic system. In: *Airborne resistivity mapping*, Vol. Paper 86-22 (ed. G.J. Palacky), pp. 63-70. Geological Survey of Canada.

Duncan, A., P Roberts, G., Buselli, G., Pik, J., Williamson, D., Roocke, P., Thorn, R. & Anderson, A. 1992. SALTMAP ? airborne EM for the environment. *Exploration Geophysics* **23**, 123-126.

Effersø, F., Auken, E. & Sørensen, K.I. 1999. Inversion of band-limited TEM responses. *Geophysical Prospecting* **47**, 551-564.

Huang, H. & Fraser, D.C. 2002. Dielectric permittivity and resistivity mapping using high-frequency, helicopter-borne EM data. *Geophysics* **67**, 727-738.

Kurtz, R.D., Macnae, J.C. & West, G.F. 1989. A controlled-source, time-domain electromagnetic survey over an upthrust section of Archean crust in the Kapuskasing Structural Zone. *Geophysical Journal International* **99**, 195-204.

Lane, R., Plunkett, C., Price, A., Green, A. & Hu, Y. 1998. Streamed data - a source of insight and improvement for time domain airborne EM. *Exploration Geophysics* **29**, 16-23.

Leggatt, P.B. 1996. Some algorithms and code for the computaiton of the step response secondary emf signal for the Spectrem AEM system. PhD thesis, Witwatersrand.

Macnae, J., King, A., Stolz, N., Osmakoff, A. & Blaha, A. 1998. Fast AEM data processing and inversion. *Exploration Geophysics* **29**, 163-169.

Spies, B. & Frischknecht, F. 1991. Electromagnetic Sounding. In: *Electromagnetic methods in applied geophysics*, Vol. 2 (ed. M. Nabighian), pp. 285-411. SEG.

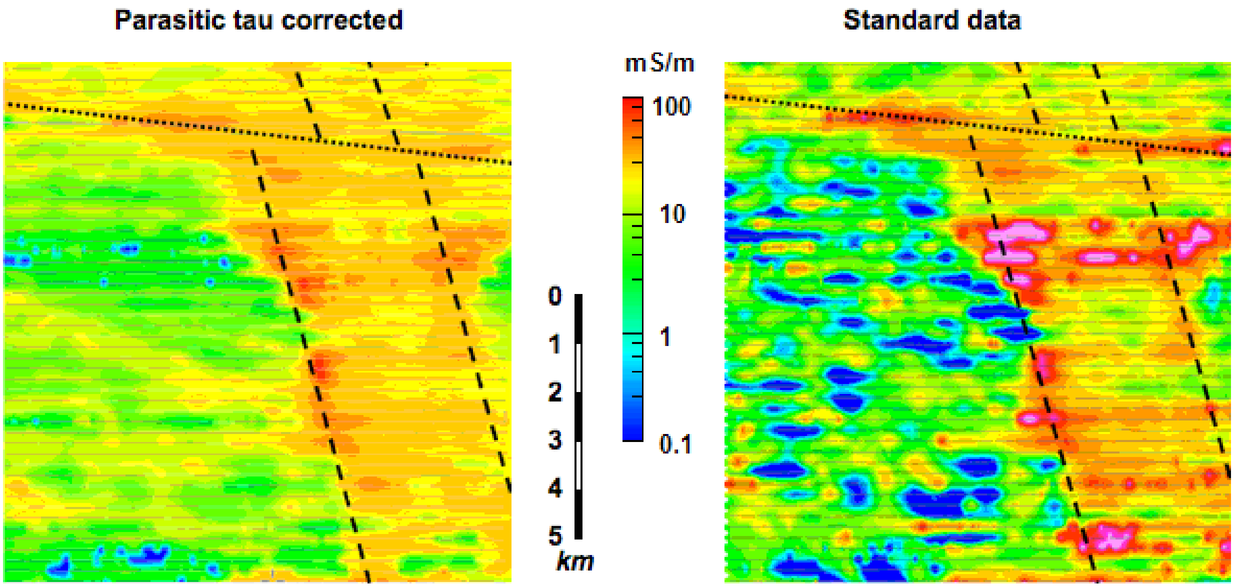

Figure 9: Comparison of mapped near-surface conductivity (average in top 10 m) compiled from EMFlow processing, showing the improvements in coherency on the left compared to uncorrected data on the right.